JOURNAL OF SOLID STATE CHEMISTRY **34**, 315–322 (1980)

A Kinetic Study of the System γ-AlOOH/Al_2O_3

S. J. WILSON* AND J. D. C. MC CONNELL

Department of Mineralogy and Petrology, University of Cambridge, Cambridge, England

Received September 24, 1979

A time–temperature study has been made of the system: γ-AlOOH (boehmite)/Al_2O_3. The isothermal TTT diagram produced demonstrates the course of the transformation sequence, which involves a number of metastable transition alumina intermediate phases. This type of treatment allows calculation of kinetic parameters for the various transformation processes, and these may be correlated with the mechanisms operating. Kinetic aspects of variations in microstructure and crystal structure have also been studied. In particular, the progress of cation migration processes involved in the transformation γ- → δ-Al_2O_3 has been followed in terms of the continuous variation of the spinel subcell parameters.

Introduction

The dehydration of boehmite (γ-AlOOH) in air does not immediately result in the formation of the thermodynamically stable form of aluminium oxide, α-Al_2O_3 (corundum), but rather produces a series of metastable, highly porous oxide phases, known as transition aluminas, before final conversion to α-Al_2O_3.

$$\gamma\text{-AlOOH} \rightarrow \gamma\text{-} \rightarrow \delta\text{-} \rightarrow \theta\text{-} \rightarrow \alpha\text{-}Al_2O_3$$

The structures of these transition aluminas are based on cubic close-packing of the oxygen anions: γ-Al_2O_3 has a tetragonally distorted defect spinel structure (*1*, *2*); δ-Al_2O_3 has a tetragonal superstructure of the spinel lattice with one unit cell parameter tripled (*1*); and θ-Al_2O_3 has the monoclinic structure of β-Ga_2O_3 (*3–6*). The structural differences between these phases thus involve only the arrangement of cations in an approximately cubic close-packed oxygen array. The transformations between the phases have been found to be topotactic (*1*, *2*, *4*, *7*).

Previous studies aimed at providing a full description of the system γ-AlOOH/Al_2O_3 have operated predominantly at the single-crystal level. Information has appeared, derived predominantly from electron microscope and diffraction studies, relating to structural and orientational aspects of the transformation sequence: boehmite → γ- → δ- → θ-Al_2O_3 (*1*, *2*, *4*, *6*, *7*); the mechanism of the dehydration step, boehmite → γ-Al_2O_3 (*8*); and the development and evolution of the morphology of the porous microstructure along the reaction sequence (*7–9*). It is apparent that there are very close links between the sequences of structural and microstructural changes.

The successive formation of the three metastable, transition alumina phases, γ-, δ- and θ-Al_2O_3, reveals the extent to which the system is controlled by the kinetics of

---

* To whom correspondence should be sent.

0022-4596/80/120315-08$02.00/0

the various transformation processes. The aim of the present work is to demonstrate the usefulness of a time–temperature treatment in providing a kinetic description of an inorganic solid-state system involving metastable behavior. The behavior will be studied at a number of levels, namely, those of crystal structure and microstructure as well as that of the phase assemblages characteristic of particular time–temperature treatments.

Experimental

The well-crystallized boehmite used in this study was CERA hydrate, supplied by The British Aluminium Company Ltd., which had a maximum crystal size of about 5 μm. Material for examination was furnace fired in air in platinum crucibles. Characterization was by X-ray diffraction, using a Philips powder diffractometer with Cu*Kα* radiation, and by transmission electron microscopy, using a Siemens 102 instrument.

Results

Phase Assemblages

Phase assemblage data obtained from about 80 isothermal firings of boehmite have been collected in the time–temperature-transformation (TTT) diagram of Fig. 1. The contours delineating the phase regions have been drawn to represent the presence of 5% of an appearing phase, or a remainder of 5% of a disappearing phase, the proportions of phases present having been estimated from X-ray powder intensities The diagram shows clearly the succession of phases observed.

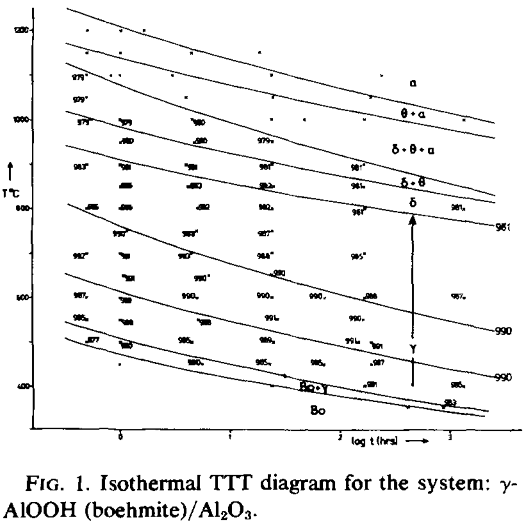

FIG. 1. Isothermal TTT diagram for the system: γ-AlOOH (boehmite)/Al_2O_3.

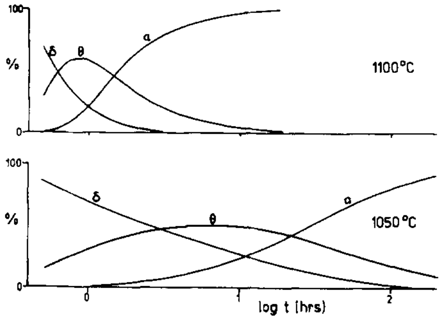

FIG. 2. Proportions of succeeding phases, for isothermal treatment at two temperatures.

The transformations δ- → θ- → α-Al_2O_3 may be seen to be quite slow with, for example, the time between first appearance of θ- and final disappearance of δ-Al_2O_3 at 1000°C taking of the order of 8 weeks. This sluggishness leads to the appearance of the important three-phase region, δ- + θ- + α-Al_2O_3. The proportions of these three phases present after firings at two representative temperatures are shown in Fig. 2. The convergence of the contours representing the appearance of θ- and of α-Al_2O_3 indicates that, for very long firings at low temperatures, a two-phase region, δ- + α-Al_2O_3, may appear, suggesting that there may be a contribution from the direct transformation δ- → α-Al_2O_3.

The X-ray powder pattern and unit cell parameters of the θ-Al_2O_3 phase were not found to vary with the time–temperature conditions of its formation. The pattern is given in Table I, and has been indexed on the basis both of the true monoclinic cell and of the pseudo-orthorhombic cell which emphasizes the similarity of the structure of θ-Al_2O_3 to the spinel superstructure of δ-Al_2O_3 (7). The unit cell parameters found for θ-Al_2O_3 by least-squares refinement are as follows (with standard deviation in the last figure quoted):

monoclinic: $a = 5.620\ (2)$
$A2/m$ $b = 2.906\ (1)$
$c = 11.790\ (5)$ Å
$\beta = 103.79\ (1)^\circ$
pseudo-orthorh.: $a = 5.620\ (2)$
$b = 2.906\ (1)$
$c = 22.90\ (1)$ Å

Both the pattern and the parameters compare well with those found by Yamaguchi *et al.* (*6*) for θ-Al_2O_3 prepared hydrothermally from η-Al_2O_3.

A previous single-crystal electron diffraction study (7) found that the structural changes involved in the $\delta \rightarrow \theta$ transformation occur gradually, and that intermediate stages could be observed. These intermediates, although undoubtedly important, cannot be observed in X-ray powder patterns since they appear as δ- + θ-Al_2O_3 mixtures. However, the similarly gradual nature of the $\gamma \rightarrow \delta$ transformation is apparent in X-ray powder patterns and the progress of this transformation may be investigated by following the gradual appearance of spinel superstructure reflections, and changes in the tetragonal distortion of the basic spinel subcell.

As a measure of this tetragonal distortion the ratio c/a for γ-Al_2O_3 phases was calculated from the positions and degree of splitting of the pairs of reflections 400/004 and 440/404, and the equivalent $c/3a$ for δ-Al_2O_3 phases from 400/00.12 and 440/40.12. The values obtained ($\times 10^3$) have been included in Fig. 1 together with contours corresponding to $c/a = 0.990$ and 0.981. The accuracy in these c/a values is about ± 1 in the last figure quoted, decreasing to about ± 2 for the most-nearly cubic phases. A preliminary report of variations in c/a ratio has appeared (*8*) but the reworking here of data for a much larger number of samples allows a more complete picture of the behavior to be presented. The c/a ratios show a continuous variation from the tetragonally distorted γ-Al_2O_3 phase first formed on the dehydration of boehmite to a nearly cubic phase, followed by a further increase in distortion as the transformation to δ-Al_2O_3 proceeds.

This continuous variation of c/a suggests that the structural changes involved in the $\gamma \rightarrow \delta$ transformation occur very gradually. Thus it is difficult to assign a single-phase δ-Al_2O_3 region on the TTT diagram. However, the gradual appearance of superstructure reflections in X-ray powder patterns, and the appearance of well-developed δ-Al_2O_3 single-crystal electron diffraction patterns, suggest that the tripled spinel superstructure of δ-Al_2O_3 is quite well developed in samples for which c/a has decreased to about 0.981.

Diagnostic regions of the diffractometer traces of a number of representative samples are shown in Fig. 3. These illustrate the variations in the degree of distortion of the spinel subcell and also the gradual appearance of the δ-Al_2O_3 superstructure reflections, most noticeably 118 and 222. They also demonstrate a reduction in reflection half-width as the transformation proceeds.

Unit cell parameters for the basic spinel subcell have been calculated for 75 samples containing γ- or δ-Al_2O_3 phases and are plotted against c/a in Fig. 4. The fit to these curves is equally good for phases in the tetragonal → cubic region and in the cubic → tetragonal region, this being a result of the small variation in cell volume over the whole range of γ- and δ-Al_2O_3 phases. Unit cell parameters representative of the c/a variations in the $\gamma \rightarrow \delta$ region of the TTT diagram may be quoted as follows:

The most tetragonal γ-Al_2O_3 phase observed was that in the sample fired at 500°C for $\frac{1}{2}$ hr with $a \simeq 7.97$, $c \simeq 7.79$ Å,

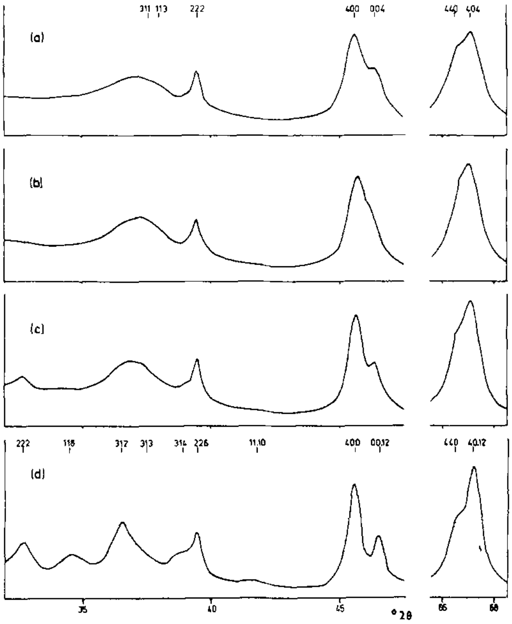

FIG. 3. X-Ray powder diffractometer traces, Cu*Kα* radiation, for samples of boehmite treated as follows: (a) 500°C 4½ hr: γ-Al_2O_3; $a = 7.954$, $c = 7.834$ Å; $c/a = 0.985$. (b) 700°C 1 hr: γ-Al_2O_3; $a = 7.936$; $c = 7.865$ Å; $c/a = 0.991$. (c) 700°C 1 week: γ-/δ-Al_2O_3; subcell $a = 7.953$, $c = 7.833$ Å; $c/a = 0.985$. (d) 800°C 8 weeks: δ-Al_2O_3; $a = 7.961$, $c = 23.43$ Å; $c/3a = 0.981$.

$c/a = 0.977$, although a reduction in the degree of interference from boehmite reflections in the powder pattern allows data for the sample 450°C $5\frac{2}{3}$ hr, $a = 7.962$, $c = 7.801$ Å, $c/a = 0.980$, to be quoted with more precision.

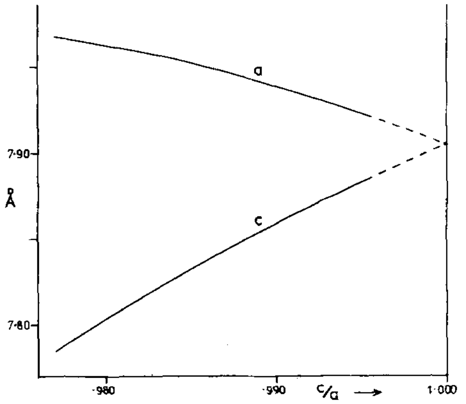

FIG. 4. Variation of spinel subcell parameters for γ- and δ-Al_2O_3 phases.

TABLE I

θ-Al_2O_3: X-RAY POWDER DATA

I	d_{obs} (Å)	Monoclinic *hkl*	Pseudo-orthorh. *hkl*	d_{calc} (Å)
6	5.45	100	101	5.46
10	4.54	$10\bar{2}$	103	4.53
60	2.860 2.823	004 $10\bar{4}$ 011	008 107 012	2.863 2.827 2.817
100	2.730	200 $20\bar{2}$	202	2.729
25	2.562	$11\bar{1}$	111	2.565
60	2.448	111	113	2.445
45	2.312	104 013	109 016	2.318 2.312
35	2.260	202 $20\bar{4}$	206	2.263
55	2.020	$21\bar{1}$	210	2.020
35	1.908	006 211 $21\bar{3}$	00.12 214	1.908 1.905
15	1.799	015	01.10	1.799
6	1.776	204 $20\bar{6}$	20.10	1.775
5	1.734	$30\bar{4}$	305	1.734
8	1.621	302 115	307 11.11	1.626 1.621
6	1.571	$31\bar{1}$	311	1.571
25	1.543	$31\bar{3}$	313	1.542
8	1.508	$30\bar{6}$	309	1.509
15	1.487	311	315	1.489
30	1.453	$11\bar{7}$ 020	11.13 020	1.455 1.453
7	1.426	017	01.14	1.425
75	1.388	215 $21\bar{7}$	21.12	1.387

The most nearly cubic γ-Al_2O_3 phase observed was that in a sample fired sequentially for 1 day at 400°C, then for 1 day at 600°C, and had $a = 7.923$, $c = 7.884$ Å, $c/a = 0.995$. Extrapolation of the curves in Fig. 4 suggests that an ideally cubic γ-Al_2O_3 would have $a = 7.906$ Å.

For δ-Al_2O_3 with $c/3a = 0.981$ the parameters found were $a = 7.961$, $c = 23.43$ Å. Further development of the superstructure results in a greater tetragonal distortion. However, the appearance of θ-Al_2O_3 causes interferences and the most tetragonal δ-Al_2O_3 found had $a = 7.964$, $c = 23.39$ Å, $c/3a = 0.979$.

Microstructure

The character of the porous microstructure developed at various stages of the transformation sequence has been described previously (*7–9*). Since in any sample there will be present crystals at various stages of the sequence, the microstructures observed will be characteristic of a particular stage rather than of the sample as a whole. Nevertheless, within the limitations imposed by sample inhomogeneity, an attempt was made in the present study to examine the time–temperature behavior of microstructure, that is, to determine whether the nature of the microstructure of a particular phase, in terms of pore size and morphology, is dependent on its preparation route. However, no obvious variation in microstructure was observed for δ-Al_2O_3 prepared in the range 800–1000°C; for θ-Al_2O_3 prepared in the range 1000–1200°C; or for the lamellar porous γ-Al_2O_3 first formed on the dehydration of boehmite at temperatures in the range 350–700°C. Furthermore δ-Al_2O_3 prepared by firing sequentially for 1 week at 400°C, then 1 week at 800°C, was indistinguishable microstructurally from δ-Al_2O_3 prepared isothermally at 800°C.

The structural and microstructural characteristics of the $\theta \rightarrow \alpha$-$Al_2O_3$ transformation will be the subject of a future publication. However, from microstructural information obtained so far, it is clear that this transformation is nucleated.

Kinetics

The information contained in the TTT diagram of Fig. 1 may be replotted to allow calculation of kinetic parameters. In an Arrhenius type plot of ln t^{-1} against $1/T$ (where t^{-1} represents a rate function), straight lines representing the contours of Fig. 1 illustrate the temperature dependence of the rates of the various transformation processes involved. Accordingly, in Fig. 5 the best possible straight lines have been drawn to represent 5% appearance and remanence of the phases, and c/a ratio contours. Energy values corresponding to the slopes of each contour have been calculated and are included in Fig. 5. The accuracy in these calculated activation enthalpies is probably no better than ±20 kJ/mole.

Discussion

The use of a time–temperature treatment has been shown, in this study, to allow investigation of kinetic behavior, at a number of levels, of a system involving several successive transformations. The levels examined are those of phase assemblages, microstructure, and crystal structure.

At the level of phase assemblages, the TTT diagram of Fig. 1 may be viewed as a nonequilibrium phase diagram. The varying slopes of the contours delineating the various phase regions suggest that there may be some dependence of the transformation sequence on route. Thus whereas in the time–temperature range studied, α-Al_2O_3 is

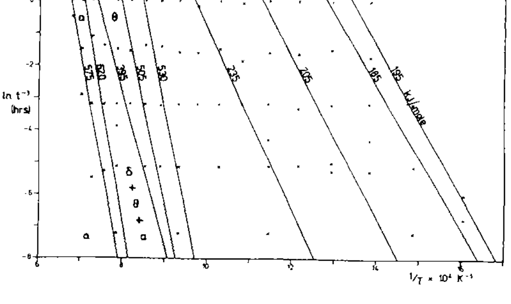

FIG. 5. Arrhenius plot of time–temperature data.

observed to succeed θ-Al_2O_3, extrapolation of Figs. 1 and 5 indicates that for very long firing times at temperatures below about 750°C, α-Al_2O_3 would nucleate directly from δ-Al_2O_3. Similarly with very short firing times at temperatures above about 1250°C it might be possible to obtain pure θ-Al_2O_3.

No evidence was found of any dependence of microstructure on route. Thus, the sequence of microstructural evolution is independent of temperature, only the rate at which it takes place being affected. Information previously obtained (*7*) on the microstructures characteristic of various stages of the transformation sequence could be superimposed on Fig. 1, to allow control and prediction of the nature of the porosity of the material.

At the structural level, clear evidence of the gradual nature of the $\gamma \rightarrow \delta$ transformation was found from the continuous variations of spinel subcell parameters, and from the gradual appearance of superstructure reflections in X-ray powder patterns. Thus there seems to be no distinct dividing line between γ- and δ-Al_2O_3 and it may be wondered whether the use of separate terminology is meaningful. However, the assignments probably do represent two ideal structure types, with γ-Al_2O_3 as a defect spinel in which the vacancies are distributed randomly, whereas in δ-Al_2O_3 the vacancies are ordered on octahedral sites, giving a spinel superstructure (*1, 7*). The variations in c/a ratio allow the progress of the cation migration processes involved in the $\gamma \rightarrow \delta$ transformation to be followed.

The mechanism proposed for the dehydration of boehmite (*8*) suggests that in γ-Al_2O_3, as first formed, the vacancies are predominantly on tetrahedral cation sites of the spinel structure. The tetragonal distortion of this early γ-Al_2O_3 will be a result of the anisotropic nature of the mechanism and also reflects the strongly anisotropic lamellar microstructure observed at this stage. Thus the change in c/a towards a more cubic phase represents the gradual formation of a more ideal γ-Al_2O_3 phase with random vacancies. Apparently, the attainment of cubic γ-Al_2O_3 suggested by extrapolation of Fig. 4, is never quite achieved, since a process of ordering of vacancies on octahedral sites, with the resultant increase in tetragonal character and gradual development of the superstructure of δ-Al_2O_3, takes over. These cation ordering processes are also reflected by variations in line width observed in the X-ray powder patterns, which may be compared with streaking effects observed in single crystal electron diffraction patterns (*8, 9*).

The large range of unit cell parameters observed here for γ-Al_2O_3, together with the obviously strong links between dehydration mechanism, microstructure and crystal structure, sheds some light on the general question of the identification of transition alumina phases from X-ray powder patterns. As an example, the phase η-Al_2O_3, encountered during the dehydration of bayerite (*1*), is a defect spinel distinguished from γ-Al_2O_3 only by slight differences in X-ray powder pattern. Certainly the range of c/a ratios (0.985–0.993) observed for η-Al_2O_3 overlaps with that observed here for γ-Al_2O_3. It is probable that these two phases represent attempts at attainment of the same ideal random defect spinel structure, but from different directions, i.e., from different precursors and thus with different inherited microstructures.

The appearance of a number of metastable transition alumina phases in the γ-$AlOOH/Al_2O_3$ system indicates that the transformation sequence is kinetically controlled. The structure of the boehmite precursor, together with the mechanism of dehydration (*8*), imposes a cubic close-packed oxygen lattice on the system, and thus the sequence $\gamma \rightarrow \delta \rightarrow \theta$-$Al_2O_3$, all based on this type of anion stacking, provides a kinetically favored reaction route. The gross reorganization necessary for the nucleation of the hexagonally close-packed α-Al_2O_3 only becomes kinetically feasible at high temperatures. Microstructure has also been shown (*7*) to influence the reaction route, by virtue of its effect on the orientational characteristics of the transformations.

The presentation of phase assemblage and *c*/*a* ratio data in the form of a TTT diagram allows calculation of kinetic parameters for the various transformation contours. Because of the method of calculation the activation enthalpy data shown in Fig. 5 should not be expected to be of high precision. However, a figure of 190 kJ/mole for the activation energy for the dehydration of boehmite to γ-Al_2O_3, obtained by Rouquerol *et al.* (*10*) by the more precise method of controlled decomposition rate thermal analysis (*11*) provides a favorable comparison with the values found in this study. The activation enthalpy data shown in Fig. 5 may be grouped into three ranges and analyzed in terms of the mechanisms of the corresponding transformations.

The activation enthalpies calculated for the dehydration of boehmite to γ-Al_2O_3, and for the transformation tetragonal → cubic γ-Al_2O_3, lie close together within the range 185–205 kJ/mole. Thus the mechanisms of the two transformations may involve similar rate-determining steps. The atomic processes involved in the transformation tetragonal → cubic γ-Al_2O_3 are solely those of migration of Al cations. Similarly, a mechanism for the dehydration of boehmite, involving countermigration of protons and Al cations, has been proposed on the basis of structural and microstructural evidence (*8*). The activation enthalpies found in this present study thus provide further support for this mechanism, and, moreover, suggest that the Al diffusion is rate determining.

Energies calculated for the contours corresponding to appearance and disappearance of δ- and θ-Al_2O_3 lie within the range 505–620 kJ/mole. Interpretation of these values may be complicated by the consecutive reaction character of the transformation sequence in this region (Fig. 2), especially if the direct transformation δ- → α-Al_2O_3 is of some importance. The contours for the disappearance of δ- and θ-Al_2O_3 will be particularly affected by such complications. However, the energy range quoted probably provides a good guide to the activation enthalpies of the transformations γ- → δ-Al_2O_3 and δ- → θ-Al_2O_3. Since these transformations are topotactic and the structures all based on cubic close-packed anion lattices, the mechanisms should again involve predominantly processes of cation migration. However, the precise, concerted Al cation migrations required to form these ordered spinel-based structures are substantially different from those involved in the dehydration of boehmite and the reorganization of γ-Al_2O_3. It may be valid to make a comparison with the figure of 460 kJ/mole found for the activation enthalpy for the self-diffusion of Al in α-Al_2O_3 (*12*). Microstructural studies have shown (*7*) that the transformations γ- → δ-Al_2O_3 and δ- → θ-Al_2O_3 are accompanied by extensive sintering of, and changes in the morphology of the internal pore structure, both of which require substantial reorganisation of the anion lattice. Thus there may also be a contribution from this type of process to the activation energy.

The energy calculated for the contour corresponding to the appearance of α-Al_2O_3, 395 kJ/mole, is distinct from and intermediate between the two ranges quoted above. This reflects the fact that whereas the other transformations are topotactic, α-Al_2O_3 is formed by a nucleation and growth mechanism in which the most significant structural step is the reorganisation of the anion lattice to give a hexagonally close-packed array.

Extrapolation of the contours of Fig. 5 to obtain the intercepts on the ln t^{-1} axis provides a guide to the relative order of magnitude of activation entropy for the various transformation processes. The intercepts observed in fact show the same grouping and order as the activation enthalpies. Thus the activation entropies are highest for the transformations to δ- and θ-Al_2O_3 and it is this that allows the appearance of these phases in the transformation sequence in spite of the very high activation enthalpies involved. This effectively is a restatement, in energetic terms, of the fact that the structural similarities in the sequence boehmite $\rightarrow \gamma$- $\rightarrow \delta$- $\rightarrow \theta$-Al_2O_3 provide a kinetically favored reaction route prior to the formation of α-Al_2O_3.

The transition alumina sequence and the time–temperature behavior observed in this study are specific to boehmite, and, in particular, to well-crystallized boehmite, since Saalfeld (*2*) found that for boehmite prepared by hydrothermal alteration of gibbsite single crystals, δ-Al_2O_3 is absent from the sequence. It should be further emphasized that the behavior observed will be specific to the heating of boehmite in air, and will be sensitive to the conditions of thermal treatment, such as the water vapor pressure. Thus under high water vapor presures boehmite has been found (*13*) to transform directly to α-Al_2O_3, and similar behavior has been observed for the isostructural γ-FeOOH (*14*). The microstructure is also likely to be sensitive to water vapor pressure.

The use of a TTT treatment has been found in this work not only to allow study of the route of a transformation sequence, but also to provide kinetic parameters for the transformation processes and to allow study of kinetic aspects of variations in crystal structure and microstructure.

Acknowledgment

The receipt by S. J. Wilson of an award under the ICI Joint Research Scheme is gratefully acknowledged.

References

1. B. C. Lippens and J. H. de Boer, *Acta Crystallogr.* **17**, 1312 (1964).
2. H. Saalfeld, *Clay Miner. Bull.* **3**,249 (1958).
3. J. A. Kohn, G. Katz, and J. D. Broder, *Amer. Mineral.* **42**, 398 (1957).
4. H. Saalfeld, *Neues. Jahrb. Mineral. Abh.* **95**, 1 (1960).
5. S. Geller, *J. Chem. Phys.* **33**, 676 (1960).
6. G. Yamaguchi, I. Yasui, and W-C. Chiu, *Bull. Chem. Soc. Japan* **43**, 2487 (1970).
7. S. J. Wilson, *Proc. Brit. Ceram. Soc.* **28**, 281 (1979).
8. S. J. Wilson, *J. Solid State Chem.* **30**, 247 (1979).
9. S. J. Wilson, *Mineral. Mag.* **43**, 301 (1979).
10. M. Boudellal, M. Ganteaume, F. Rouquerol, and J. Rouquerol, in preparation; J. Rouquerol, personal communication.
11. J. Rouquerol, *J. Therm. Anal.* **5**, 203 (1973).
12. A. E. Paladino and W. D. Kingery, *J. Chem. Phys.* **37**, 957 (1962).
13. R. S. Bradbeer and A. C. D. Chaklader, *Sci. Ceram.* **7**, 551 (1973).
14. R. Giovanoli and R. Brutsch, *Thermochim. Acta* **13**, 15 (1975).